Theoretical modeling of UV-Vis absorption and emission spectra in liquid state systems including vibrational and conformational effects: The vertical transition approximation

Maira D'Alessandro, Massimiliano Aschi, Claudia Mazzuca, Antonio Palleschi, and Andrea Amadei

Citation: J. Chem. Phys. **139**, 114102 (2013); doi: 10.1063/1.4821003
View online: http://dx.doi.org/10.1063/1.4821003
View Table of Contents: http://jcp.aip.org/resource/1/JCPSA6/v139/i11
Published by the AIP Publishing LLC.

Theoretical modeling of UV-Vis absorption and emission spectra in liquid state systems including vibrational and conformational effects: The vertical transition approximation

Maira D'Alessandro,[1] Massimiliano Aschi,[1,a)] Claudia Mazzuca,[2] Antonio Palleschi,[2] and Andrea Amadei[2,a)]
[1]*Dipartimento di Scienze Fisiche e Chimiche, Università dell'Aquila, Via Vetoio s.n.c., 67100 L'Aquila, Italy*
[2]*Dipartimento di Scienze e Tecnologie Chimiche, Università di Roma 'Tor Vergata,' Via della Ricerca Scientifica 1, 00133 Rome, Italy*

(Received 25 July 2013; accepted 28 August 2013; published online 17 September 2013)

In this paper we describe in detail a general and efficient methodology, based on the perturbed matrix method and molecular dynamics simulations, to model UV-Vis absorption and emission spectra including vibrational and conformational effects. The basic approximation used is to consider all the chromophore atomic coordinates as semiclassical degrees of freedom, hence allowing the calculation of the complete spectral signal by using the electronic vertical transitions as obtained at each possible chromophore configuration, thus including the contributions of vibrations and conformational transitions into the spectrum. As shown for the model system utilized in this paper, solvated 1-phenyl-naphthalene, such an approximation can be rather accurate to reproduce the absorption and emission spectral line shape and properties when, as it often occurs, the vertical vibronic transition largely overlaps the other non-negligible vibronic transitions. © *2013 AIP Publishing LLC*. [http://dx.doi.org/10.1063/1.4821003]

INTRODUCTION

The reproduction and interpretation of the absorption and fluorescence spectra of molecular systems in condensed phase is an active research field of contemporary theoretical-computational chemistry. In particular fluorescence signal, due to its extreme sensitivity to conformational transitions, has become in the recent years an efficient and widely utilized tool for describing the complex micro environments surrounding the chromophores.[1] For these reasons theoretical-computational approaches should be able to reproduce not only the position of the spectral maxima but also the related line shapes.[2,3] It follows that the simulation of the absorption or fluorescence spectra in realistic conditions basically relies on (i) the possibility of studying the electronic excited states of medium-large size molecular systems at each possible conformational state, (ii) the possibility of including both the quantum and semiclassical vibrations of the chromophore, and (iii) the possibility of properly treating the interaction of the chromophore with the surrounding atomistic environment. In the last decade, mainly because of the computer power increase and the development of accessible electronic-structure methods for treating excited states,[4–8] several research groups[9–20] have proposed efficient theoretical-computational methods and, hence, reliable calculations of the absorption or fluorescence spectra for rigid or semi-rigid species in condensed phase are nowadays feasible. However, in spite of the important advances in this field, additional work is necessary in particular for complex systems such as solutions and bio-macromolecules. In these cases, the huge dimension of the configurational space spanned by the chromophore and the perturbing environment as well as the relevant effects of the fluctuating perturbation onto the chromophore quantum properties, require computational approaches able to properly account for the complexity of the whole system and, for the emission signal, the related long-timescale relaxations.[21] As a part of our continuous interest in the study of the quantum properties in complex molecular systems,[22–25] we describe in this study a general and efficient methodology, based on the perturbed matrix method and molecular dynamics simulations, to model UV-Vis absorption and emission spectra of complex molecular systems including vibrational and conformational effects. As a case study we have selected the UV-Vis absorption-fluorescence spectra of 1-phenyl-naphthalene (1PN, Figure 1) in solution.

This molecule belongs to the general class of Polycyclic Aromatic Hydrocarbons (PAH) with low molecular weights which are extensively studied and used as organic electronics building blocks, representing a class of fluorescent compounds with promising properties in the field of industrial applications. In particular, in this study we focus our attention on the 1PN spectral signals involving the ground state S_0 and first spectroscopic accessible excited state S_1 defined, as in other works in this field,[26,27] as the lowest energy excited state characterized by a non-negligible transition dipole. Our approach, based on the use of the Perturbed Matrix Method (PMM)[28,29] in conjunction with Molecular Dynamics (MD) simulations and Time-Dependent Density Functional Theory (TD-DFT) methods[30,31] is essentially inspired by the previous works in this field, in particular concerning the explicit parametrization of the excited states.[26,27] However, unlike other

a)Authors to whom correspondence should be addressed. Electronic addresses: massimiliano.aschi@univaq.it and andrea.amadei@uniroma2.it.

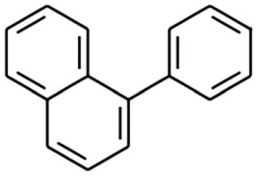

FIG. 1. Schematic view of 1-phenyl-naphthalene.

computational approaches, the method presented in this study is aimed at explicitly including the fluctuating perturbation of the surrounding environment maintaining as intact as possible the chromophore configurational complexity, both expected to play a key role in the correct determination of the spectral maximum position and line shape. In previous works, we have used the PMM-MD approach to model absorption spectra also including the effects of possible conformational transitions and/or local configurational fluctuations.[32] Moreover for the case of a very simple molecule (i.e., carbon monoxide) we showed how to use PMM-MD to reconstruct rigorously instantaneous quantum vibrational states and their coupling to the instantaneous electronic states involved in the vibronic transitions.[23] However such kind of PMM-MD calculations, although in principle always possible, are computationally very expensive and for any interacting molecule characterized by more than one or at most just a few vibrational modes such calculations become computationally prohibitive and, therefore, some kind of general and still reasonably rigorous approximation is mandatory.[24] In fact, a general computationally feasible PMM-MD based methodology to model both the absorption and emission spectra due to electronic transitions including the vibrational and conformational effects was not yet introduced. In this paper we describe in detail a general and reasonably rigorous PMM-MD approach based on the approximation of treating all the chromophore internal vibrations as semiclassical, thus explicitly including, within such a level of approximation, all the vibrational-conformational effects in the calculation of the vibronic absorption and, for the first time with the use of PMM, the emission spectra.

THEORETICAL METHOD

General considerations

The present study is based on the application of PMM and MD simulation. The theoretical basis of the PMM-MD method is reported elsewhere[28,29] and, hence, we only provide a brief report just remarking some key aspects for modeling spectral signals, in particular in the evaluation of the emission spectrum and related observables.

PMM-MD, essentially originating from the perturbation-theory, similar to the most popular QM/MM methods[33,34] is based on the determination of the quantum states of a predefined portion of a complex atomic-molecular system, e.g., the solute (hereafter termed as Quantum Centre, QC) interacting with the environment, e.g., the solvent molecules.

The main peculiarity of this method is to preserve, as much as possible, both the configurational complexity of the system and a good definition of the quantum observables of the perturbed QC.

For this purpose the system, e.g., the solute and the solvent, is first simulated by MD simulation in order to exhaustively explore the related configurational space. Then, after a careful and critical selection of the QC (in general – but not necessarily always – the solute molecule) a set of unperturbed (gas-phase) electronic states Φ_l^0 is evaluated using standard quantum-chemical calculations. In the simplest case the QC is a rigid (i.e., no semiclassical internal coordinates) or semi-rigid (i.e., the semiclassical internal coordinates only provide vibrations around the mean structure) species, hence not involving conformational transitions. In such a condition the unperturbed states are evaluated only at a single semiclassical QC geometry corresponding to the QC mean structure (reference structure) as obtained by the MD simulation, i.e., averaging over the semiclassical vibrations, with the quantum vibrational degrees of freedom relaxed at their unperturbed minimum energy positions. This means that at each MD frame we use the minimum energy positions of the quantum vibrational coordinates as obtained for the unperturbed QC, at the semiclassical reference geometry, in its electronic state best corresponding to the perturbed QC electronic state involved in the MD simulation (for the *i*th perturbed state typically, but not always, the *i*th unperturbed state). Note that (i) for fluid-liquid state systems at ordinary temperatures the molecular rototranslational coordinates can be considered as semiclassical degrees of freedom; (ii) for all the electronic states of interest we assume the same semiclassical internal coordinates, i.e., for each electronic state the corresponding quantum vibrational modes are defined within the same configurational subspace; (iii) the environment perturbation provides variations of the minimum energy positions which are negligible for electronic state calculations, hence allowing the use of the unperturbed positions; (iv) we always consider the absorption or emission process as starting from the electronic ground or excited state in its vibrational ground state, i.e., with relaxed quantum vibrational modes.

When a flexible QC is concerned, a collection of unperturbed electronic states Φ_l^{0-j} is calculated for each QC *j*th sampled conformation at the corresponding reference structure, termed as Representative Configuration (RC) extracted through a clustering-procedure (see the Computational Methods section), with each conformation hence equivalent to a semi-rigid QC.

Finally, for both the above cases, the QC perturbed electronic states are simply provided by diagonalizing at each frame of the MD simulation, the QC electronic Hamiltonian including the environment perturbation and built with the unperturbed basis set (Φ_l^0 or Φ_l^{0-j}), hence providing a "trajectory" of perturbed electronic energies and eigenvectors, which can be used for determining any observable value of interest. Therefore, in the case of a flexible QC at each MD step, the Root Mean Square Deviation (RMSD) of the instantaneous QC configuration with respect to all the extracted RCs is performed. Hence, when at a given MD frame the minimum value of RMSD is found corresponding to the ξth RC, we construct the frame-perturbed QC Hamiltonian matrix using the unperturbed basis set $\Phi_l^{0-\xi}$ determined by the quantum-

chemical calculations on the gaseous ξth RC. Diagonalization of such a perturbed Hamiltonian matrix produces the instantaneous perturbed Hamiltonian eigenstates and eigenvalues. This procedure is repeated at each frame of the simulation and the results are concatenated providing a properly weighted trajectory of perturbed eigenstates and related properties (e.g., the perturbed electric dipoles), now including the possible effects of conformational transitions. Note that in the above procedure the MD simulation employed to obtain the absorption signal must be performed within the electronic ground-state ensemble (ground state force field), while when the emission signal is concerned a QC electronic excited state MD simulation should be used. Making use of the ergodic hypothesis, from the distribution of the instantaneous electronic excitation energies and corresponding transition dipoles obtained, as previously described, by the MD trajectory we can reconstruct the electronic vertical absorption or emission spectrum determining the vibronic vertical absorption or emission spectral signal (i.e., the vibronic spectrum maximum and most of the related broadening).

Explicit modeling of vibrational and conformational effects: The vertical transition approximation

For a chromophore with the vibronic vertical spectral signal broad enough to include within its frequency range all the other non-negligible vibronic transitions, the overall vibronic line-shape can be typically well approximated by the electronic vertical transition spectrum, considering the quantum vibrational coordinates as semiclassical high-frequency modes which hence are always virtually constrained to their minimum energy positions.

Such a basic approximation, equivalent to modeling the vibrational effects on the spectral line-shape as only due to semiclassical degrees of freedom, is reasonably accurate as the vertical vibronic transition frequencies are typically almost identical to the corresponding electronic vertical transition frequencies and the missing lowering of the spectral intensity due to quantum vibrational averaging of the transition dipole is roughly compensated by the lack of summation of the vertical vibronic signal with the other non-negligible vibronic transition signals.

Within such a model, for an infinitely diluted chromophore in a liquid-state system, the complete spectrum can be expressed via either the extinction coefficients for the $0\rightarrow i$ electronic excitation $\varepsilon_{0,i}(\nu)$ or the emission rates for the $0\rightarrow i$ electronic relaxation $k_{i,0}(\nu)\rho(\nu)$, given by

$$\varepsilon_{0,i}(\nu) = \frac{|\boldsymbol{\mu}_{o,i}|_{\nu}^2 \rho(\nu) h\nu}{6c\varepsilon_0\hbar^2}, \tag{1}$$

$$k_{i,o}(\nu)\rho(\nu) = 8\pi h \frac{|\boldsymbol{\mu}_{o,i}|_{\nu}^2}{6c\varepsilon_0\hbar^2}\left(\frac{\nu}{c}\right)^3 \rho(\nu), \tag{2}$$

where ε_0 is the vacuum dielectric constant, c is the vacuum light speed, h is the Planck constant, $\hbar = \frac{h}{2\pi}$, $|\boldsymbol{\mu}_{o,i}|_{\nu}^2$ is the mean electronic transition dipole square length as obtained averaging within the ν, $\nu + d\nu$ frequency interval, and $\rho(\nu)$ is the probability density of the vertical transition frequency of a single QC embedded in a large atomic-molecular environment, due to the combined effects of environment perturbation, semiclassical vibrations, and conformational transitions. Once again it is worth to note that in the previous equations $|\boldsymbol{\mu}_{o,i}|_{\nu}^2$ and $\rho(\nu)$ when used to provide the absorption signal (Eq. (1)) refer to the electronic ground state ensemble, while when the emission signal is considered (Eq. (2)) they must be evaluated within the QC electronic excited state ensemble.

Using the N frames (in principle $N\rightarrow\infty$) of the MD trajectory as a proper sampling of the QC-environment statistical ensemble state distribution we can write

$$\varepsilon_{0,i}(\nu) = \lim_{N\rightarrow\infty}\frac{1}{N}\sum_{n=1}^{N}\frac{|\boldsymbol{\mu}_{o,i}|_{ref,n}^2 \rho_n(\nu) h\nu}{6c\varepsilon_0\hbar^2}, \tag{3}$$

$$k_{i,o}(\nu)\rho(\nu) = 8\pi h \lim_{N\rightarrow\infty}\frac{1}{N}\sum_{n=1}^{N}\frac{|\boldsymbol{\mu}_{o,i}|_{ref,n}^2}{6c\varepsilon_0\hbar^2}\left(\frac{\nu}{c}\right)^3 \rho_n(\nu), \tag{4}$$

where $\rho_n(\nu)$ is the probability density of the transition frequency at the nth MD frame, i.e., only due to the semiclassical vibrations around the reference configuration corresponding to that MD frame, $|\boldsymbol{\mu}_{o,i}|_{ref,n}^2$ is the perturbed transition dipole square length at the nth MD frame as obtained for the reference configuration corresponding to that MD frame (i.e., we neglect the effects of the semiclassical vibrations on the transition dipole) and, again, the transition dipoles and the probability densities in frequency space are obtained in the electronic ground state ensemble in Eq. (3) and in the QC electronic excited state ensemble in Eq. (4).

When we deal with a completely rigid QC and hence with a fixed QC geometry in both equations

$$\rho_n(\nu) = \delta(\nu - \nu_n), \tag{5}$$

where ν_n is the perturbed electronic vertical transition frequency of the QC structure at the nth frame of the MD simulation. Differently, when dealing with a semirigid or, possibly, a flexible QC involving conformational transitions, $\rho_n(\nu)$ can be properly modeled via a Gaussian distribution centered in $\nu_{ref,n}$ (the perturbed electronic vertical transition frequency of the nth frame QC reference structure) providing

$$\rho_n(\nu) = \left(\frac{1}{2\pi\sigma_{ref,n}^2}\right)^{1/2} e^{-(\nu-\nu_{ref,n})^2/(2\sigma_{ref,n}^2)}, \tag{6}$$

with the nth MD frame variance $\sigma_{ref,n}$ given by the semiclassical vibrations around the nth frame reference structure.

Hence, provided the explicit evaluation of $\nu_{ref,n}$ and $\sigma_{ref,n}$ by insertion of Eq. (6) into Eq. (3) or (4) we can explicitly obtain the complete spectral behavior or association with the electronic transition of interest within our basic approximation (note that in the limit $\sigma_{ref,n}\rightarrow 0$ the Gaussian distribution tends to a Dirac function and, hence, Eq. (5) can be considered a special case of Eq. (6)).

In practice, in order to simplify the computational procedure it is reasonable to assume that $\sigma_{ref,n} \cong \sigma$, that is the variance is basically the same for all the possible conformations and, moreover, independent of the environment perturbation, with σ explicitly evaluated using the unperturbed QC electronic transitions for a number of configurations within a given conformation.

Within such a simplification, Eqs. (3) and (4) become

$$\varepsilon_{0,i}(\nu) \cong \lim_{N\to\infty} \frac{1}{N} \sum_{\nu_{ref}} \frac{|\boldsymbol{\mu}_{o,i}|^2_{\nu_{ref}} h\nu}{6c\varepsilon_0\hbar^2} \frac{n(\nu_{ref})}{N} \frac{e^{-(\nu-\nu_{ref})^2/(2\sigma^2)}}{\sqrt{2\pi\sigma^2}}, \tag{7}$$

$$k_{i,o}(\nu)\rho(\nu) \cong 8\pi h \lim_{N\to\infty} \frac{1}{N} \sum_{\nu_{ref}} \frac{|\boldsymbol{\mu}_{o,i}|^2_{\nu_{ref}}}{6c\varepsilon_0\hbar^2} \frac{n(\nu_{ref})}{N} \times \frac{e^{-(\nu-\nu_{ref})^2/(2\sigma^2)}}{\sqrt{2\pi\sigma^2}} \left(\frac{\nu}{c}\right)^2, \tag{8}$$

with the summation now running over the perturbed vertical transition frequencies of the reference structures discretized in a large number of tiny bins, $|\boldsymbol{\mu}_{o,i}|^2_{\nu_{ref}}$ is the reference structure mean electronic transition dipole square length obtained by averaging within the frequency bin centered at ν_{ref} and $n(\nu_{ref})$ the corresponding number of MD frames within the bin.

Finally, the overall absorption spectrum is obtained via summing over all the $\varepsilon_{0,i}(\nu)$ of interest and from the definition of the emission rate, providing the emission spectrum, we can readily obtain the fluorescence radiative constant k_r for the $i\to0$ transition simply integrating the emission signal in frequency space

$$k_r = \langle k_{i,0}(\nu)\rangle = \int k_{i,0}(\nu)\rho(\nu)d\nu. \tag{9}$$

MATERIALS AND EXPERIMENTAL METHODS

1PN was from Aldrich Chem. Co. (Sigma-Aldrich, CA, USA). Solvents were of spectroscopic grade and were acquired from Carlo Erba Reagenti (Carlo Erba reagent srl, Milano, Italy). UV-Vis absorption spectra were recorded with a Varian 100 scan UV-Vis spectrophotometer (Varian Inc., Palo Alto, USA). Steady-state fluorescence spectra were measured on a SPEX Fluorolog spectrofluorimeter (Horiba, Japan). Time-resolved experiments were performed on a CD900 single photon counting apparatus (Edinburgh Instruments, Edinburgh, UK). Nanosecond pulsed excitation was obtained with a flash-lamp filled with ultrapure hydrogen (0.3 bar, 40 kHz repetition rate; instrument pulse width: 1.2 ns). Time-resolved experiments were performed also on a Lifespec-ps Instruments Edinburg instrument, UK operating in single photon counting mode. Nanosecond pulse excitation was obtained with a NanoLED light source (298 nm, pulse excitation width: 1.0 ns 0.9 MHz repetition rate). Fluorescence intensity decays were acquired until a peak value of 10^4 counts was reached and analyzed with the software provided by Edinburgh Instruments. The decay curves were fitted by a nonlinear least squares analysis to exponential functions through an iterative deconvolution method. In particular, the decays were fitted according to the expression

$$\mathrm{I(t)} = \Sigma_\mathrm{i}\alpha_\mathrm{i} \exp(-\mathrm{t}/\tau_\mathrm{i}), \tag{10}$$

where τ_i is the *i*th decay time observed and α_i is the *i*th pre-exponential factor that represents the relative contribution of the decay to the emission intensity[35–37] From quantum yield values and decay data it is possible to obtain the radiative ($\mathrm{k_r}$) and non-radiative ($\mathrm{k_{nr}}$) constants for 1PN.[38] The solvents used, i.e., acetonitrile (ACN) and cyclohexane (CHEX) span a wide polarity range in terms of both different orientation polarizability (Δf_p) and empirical "*py* scale."[39,40] Δf_p was obtained by the static dielectric constant ε and refractive index (n) of the solvent by means of the following equation:

$$\Delta f_p = (\varepsilon - 1)/(2\varepsilon - 1) - (n^2 - 1)/(2n^2 - 1). \tag{11}$$

The empirical *py* scale of solvent polarity has been established on the basis of the emission response of pyrene. The Δf_p and the *py* values are 0.31 and 1.70; 0.00 and 0.56 for ACN, and CHEX, respectively. Fluorescence experiments were carried out in quartz cells, using solutions bubbled for 20 min, with ultrapure argon, before each measurement. Quantum yield was obtained by using a solution of 2-aminopiridine in sulfuric acid 0.1N as a fluorescence standard.[41] Emission spectra were corrected for the instrument responses. Temperature was controlled within $\pm0.1\,^\circ$C with a thermostated cuvette holder.

COMPUTATIONAL METHODS

Force field assessment

For the semi-classical simulations of the solvated molecule, an all-atoms model has been adapted from the *Gromos* force field.[42] In particular, for the ground state MD simulation (employed to obtain the absorption spectrum) due to the fact that for 1PN, as usual, the perturbed and unperturbed electronic ground states are virtually identical, we used the atomic point charges of the unperturbed ground state QC calculated by standard electrostatic fitting procedures as implemented in quantum-chemical packages (see below). The same level of theory was used to obtain the torsion angle potential energy of the unperturbed QC electronic ground state to be used within the ground state MD simulation. Note that for each RC obtained by this simulation, we employed the unperturbed electronic ground state quantum vibrational modes minimum energy positions (see below) for PMM calculations. The parametrization of the force field as well as the definition of the RC's for the QC excited state MD simulation (employed to obtain the emission spectrum) is more complex, in principle requiring a polarizable QC and the use of different unperturbed electronic states to obtain at each MD frame the proper quantum vibrational modes minimum energy positions to be used in the corresponding RC.[25,27]

However, for 1PN the first perturbed spectroscopic accessible excited state, as it is often the case, corresponds essentially to the unperturbed first excited state, as shown analyzing the electronic excitations obtained from the ground state simulation (data not shown). Moreover, such QC first unperturbed excited state is very similar to the unperturbed ground state as far as the bond lengths, bond angles, and atomic point charges are concerned thus allowing, in line with previous studies,[26,27] to use the same procedure associated with the ground state simulation to obtain the excited state force field and RC's definition with the only modifications of employing different dihedral angle potential energy and quantum vibrational coordinates minimum energy positions, with the latter in this

case obtained from the first unperturbed electronic excited state.

Molecular dynamics simulations details

The molecule has been put at the center of a dodecahedric box filled with 1000 ACN molecules at experimental density 0.786 g/cm^3 corresponding to 1.0 bar pressure at 300 K (the simulation temperature).

For the simulation we employed the standard protocol: an initial energy minimization of both solute and solvent has been carried out, then the system was gradually heated from 50 K to 300 K using short (200 ps) MD simulations. The trajectory was propagated up to 60 ns in NVT ensemble at 300 K (using the Berendsen algorithm[43] with τ equal to the time-step used for the integration algorithm, thus being equivalent to the isokinetic coupling[44] ensuring a correct configurational distribution). The LINCS algorithm[45] was employed to constrain all bond lengths and long range electrostatic interactions were computed by the particle mesh Ewald method[46] with 34 wave vectors in each dimension and a 4th order cubic interpolation. Gromacs package[47] was used for the simulation. At the end of each simulation the molecule was re-centered in the middle of the box before using the trajectory for further calculations.

Essential dynamics analysis

As anticipated in the Introduction, when the QC turns out to be a flexible species we need to evaluate different sets of unperturbed basis-set for each conformation, Φ_l^{0-j}. Therefore, it is important to extract by the MD simulation a significant number of QC-conformations utilizing a rigorous tool. As in a previous article[32] Essential Dynamics (ED) has been utilized in this study at this purpose. Without entering into the details of the method[48] we just summarize its main features: using the equilibrated MD trajectory, the QC all-atoms covariance matrix was constructed and diagonalized. Such a transformation produces a set of orthogonal eigenvectors which represent the new collective coordinates. Eigenvectors corresponding to the largest eigenvalues define the essential directions in which the largest configurational fluctuations take place. This subset of eigenvectors represents the essential-space. Hence, the projection of the trajectory onto the essential-space produces an ensemble of high-probability basins which provides the collection of significant QC conformations and related RCs.

Unperturbed quantum chemical calculations

On the basis of the reference semiclassical geometries previously extracted by ED, standard quantum-chemical calculations have been carried out on the isolated QC to obtain the different sets of unperturbed basis sets using the following protocol:

(i) A geometrical relaxation of only the internal non-classical degrees of freedom (i.e., the internal coordinates corresponding to bond stretching and bending) was carried out using B3LYP hybrid functional[49,50] in conjunction to the 6-311G* atomic basis set. This procedure was used for both the electronic unperturbed ground (S_0) and first excited state (S_1). For this purpose we used a standard internal-coordinates minimization procedure as implemented in the Gamess package.[51] Note that the same package with same level of theory was used for the force-field parametrization for both electronic states.

(ii) These locally minimized structures were then used to obtain the electronic unperturbed ground and first six excited states to be used in the PMM procedure utilizing TD-DFT[52] calculations with the same functional and basis set adopted for the minimization. For determination of the vertical excitations, TD-DFT calculations (in the linear and quadratic response approximation) were performed using the Dalton[53] program.

RESULTS AND DISCUSSION

The experimental data collected for 1PN in the different solvents are shown in Figure 2. The UV absorption of 1PN (Figure 2(a)) is characterized by two spectral bands in the 200-340 nm region, while the emission spectrum (Figure 2(b)) displays a non-structured profile centred at 344 nm. Spectroscopic information obtained by absorption and fluorescence measurements are reported in Tables I and II and they are in agreement with previously published results.[54]

The sensitivity of the 1PN spectroscopic properties to solvent polarity has also been analysed. The absorption and emission spectra in CHEX and ACN are comparable (Table I); the negligible increase in the quantum yield (see Table II) observed in the less polar solvent (CHEX) indicates that the radiative relaxation is not significantly influenced by the nature of the solvent.[55]

On the basis of the scarce sensitivity of the experimental spectral features of 1PN to the solvent polarity, we decided to use only ACN solvent for computationally reconstructing and studying the spectroscopic behavior of solvated 1PN. ED analysis of the semiclassical internal motions of this molecule

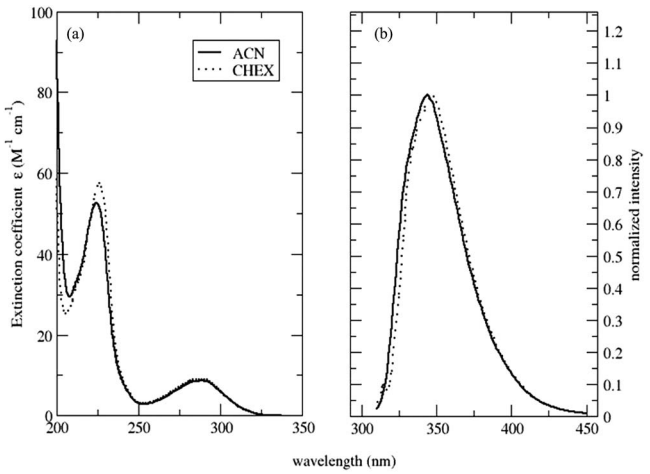

FIG. 2. Experimental spectra of absorption (a) and emission (b) of 1-PN in the different solvents.

TABLE I. Photophysical parameters of experimental absorption spectra of 1PN in different solvents.

Solvent	λ_{max} (nm)	$\varepsilon(\lambda_{max})$ (10^3 M^{-1} cm^{-1})
Acetonitrile	225 ± 1	52.4 ± 0.3
	289 ± 1	8.6 ± 0.1
Cyclohexane	226 ± 1	57.4 ± 0.2
	289 ± 1	9.0 ± 0.1

in ACN as obtained by the MD simulation at 300 K provided a single relevant conformational coordinate (associated with the first essential eigenvector), basically corresponding to the dihedral angle between the phenyl and naphthyl rings, which was used to define the different accessible conformations and related RCs. In Figure 3 we show the probability distribution of the internal coordinates fluctuations onto the first ED eigenvector as obtained for the S_0 and S_1 MD trajectories, clearly indicating that in both electronic states solvated 1PN undergoes to large semiclassical configurational fluctuations distributed according to a Gaussian-like curve (correlation coefficient with a fitted Gaussian over 0.99 in both cases).

Such a harmonic-like fluctuation behavior is not surprising when considering, as in the present case, a single conformational basin which is typically characterized by a roughly quadratic free energy profile along the conformational coordinate.

From both the ground state and first excited state simulations, we have then collected five RCs (providing five conformations) of 1PN to be used for the TD-DFT unperturbed electronic states calculations furnishing the basis sets for the PMM-MD calculations, as described in the Theoretical Method section. In Figure 4 we report the calculated absorption spectra for the $S_0 \rightarrow S_i$ ($i = 1, 2, \ldots, 6$) electronic vertical transitions in the low-energy range (λ larger than 200 nm).

From the figure it is evident that the 1PN absorption spectrum in the 220-380 nm range is largely due to the first vertical excitation with only a limited contribution of all the other considered excitations (the excitations beyond the $S_0 \rightarrow S_6$ do not contribute to the spectral line shape within the considered frequency range).

Finally, in Figure 5 we explicitly compare the calculated 1PN absorption (panel (a)) and emission (panel (b)) spectra with the corresponding experimental ones in ACN.

Remarkably, the calculated spectra reproduce almost exactly both the absorption and emission λ_{max} (see Table III) as well as the corresponding spectral shapes. Only a slight overestimation of the intensity and width is present in the calculated absorption spectrum, probably due to the approximation

TABLE II. Photophysical parameters of experimental fluorescence spectra for 1PN in different solvents. k_r and k_{nr} are the radiative and non-radiative relaxation rate constants and for such properties the relative uncertainty is about 10%.

Solvent	λ_{max} (nm)	Quantum yield	k_r (10^6 s^{-1})	k_{nr} (10^6 s^{-1})
ACN	344 ± 1	0.23 ± 0.02	24.5	81.9
CHEX	342 ± 1	0.27 ± 0.03	22.5	60.8

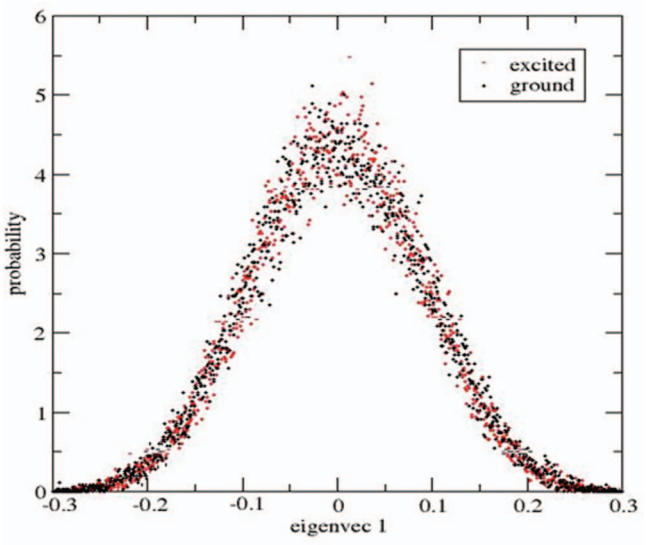

FIG. 3. Probability distributions of the S_0 and S_1 MD trajectories in ACN onto their first essential eigenvector.

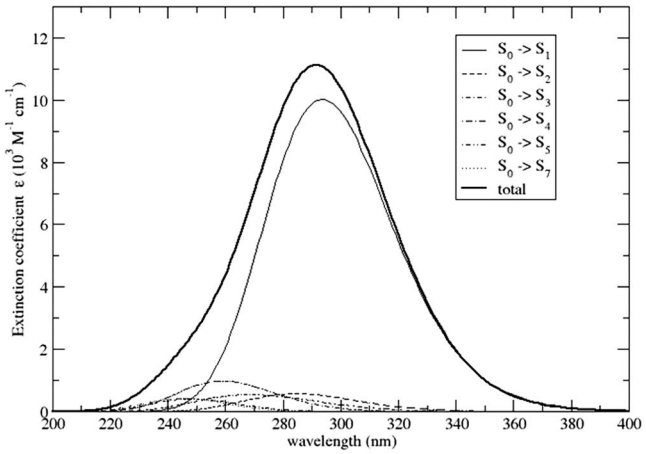

FIG. 4. PMM-MD calculated absorption signals for the $S_0 \rightarrow S_i$ (i = 1, 2, ..., 6) electronic vertical transitions of 1PN in ACN; the bold solid line is the total absorption signal as obtained from the sum of the other curves.

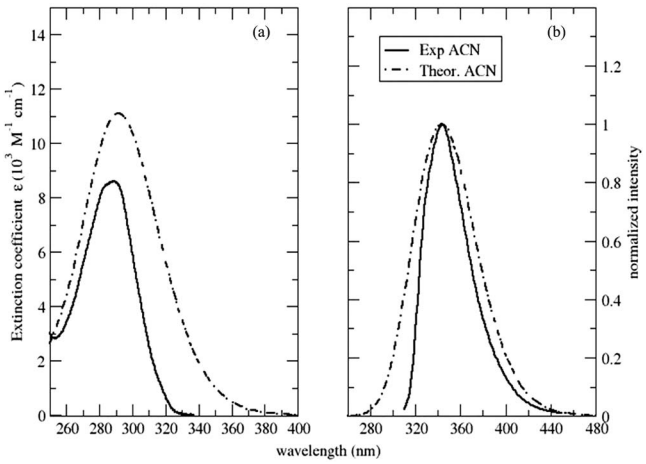

FIG. 5. Experimental and theoretical data for absorption (a) and emission (b) of 1PN in ACN.

TABLE III. Summary of spectral parameters from experimental and theoretical absorption and fluorescence signals for 1PN in ACN.

	Absorption λ_{max} (nm)	Absorption $\varepsilon(\lambda_{max})$ (10^3 M^{-1} cm^{-1})	Emission λ_{max} (nm)	$1/k_r$ (ns)
Experimental	289 ± 1	8.6 ± 0.1	344 ± 1	40.8 ± 4.0
Theoretical	291 ± 1	11.103 ± 0.018	344 ± 1	47.67 ± 0.12

of treating all the vibrational effects in terms of semiclassical degrees of freedom (see the Theoretical Method section), while the calculated fluorescence spectrum also reproduces almost exactly the experimental width (for the emission spectra we considered, as usual, a normalized intensity). As described in the Theoretical Method section the present approach is equivalent to assume always a unitary overlap integral for the vibrational wavefunctions involved in the vibronic transitions, thus possibly providing an overestimation of the spectral intensity. In general the lack of summation of the vertical vibronic signal with the other non-negligible vibronic transition signals partially compensates such an approximation, which hence typically provides a slight overestimation of the spectral signal.

Interestingly, the calculated radiative rate constant fairly well reproduces the experimental value (see Table III) indicating that also the emission spectrum intensity is rather well reproduced by the model.

CONCLUSIONS

In this article we described a general and efficient theoretical-computational approach, based on the PMM-MD method, to model in detail the complete absorption and emission spectra of a chromophore in condensed phase systems, including in the calculations the vibrational and conformational effects. The basic approximation used in the model is to consider all the chromophore atomic coordinates as semiclassical degrees of freedom, hence allowing to reconstruct the full spectroscopic signal by using the electronic vertical transitions at each possible chromophore-environment configuration. In this paper we also showed that when the vertical vibronic transition largely overlaps the other non-negligible vibronic transitions, as for the model system (1PN) utilized in this work, the theoretical model proposed fairly well reproduces the vibronic absorption or emission spectrum as well as the main related properties (e.g., the radiative rate constant). For chromophores involving relevant quantum-vibrational effects such as significant vibronic transitions well separated from the vertical one as it may occur for rigid and weakly interacting molecules, the present approach is obviously inaccurate and an explicit, although still approximated, modeling of the vibrational quantum states involved in the vibronic transitions must be used (in a future work we will address such an issue). Finally, this approach provides for the first time within the PMM-MD framework, a rigorous procedure to treat emission processes to be used in reconstructing the fluorescence spectra and related observables often representing the essential experimental information to characterize complex molecular systems.

[1] E. M. Goldys, *Fluorescence Applications in Biotechnology and Life Sciences* (Wiley-Blackwell, New Jersey, 2008).
[2] F. J. Avila Ferrer, J. Cerezo, E. Stendardo, R. Improta, and F. Santoro, J. Chem. Theory Comput. **9**, 2072 (2013).
[3] M. Biczysko, J. Bloino, F. Santoro, and V. Barone, "Time-independent approaches to simulate electronic spectra lineshapes: From small molecules to macrosystems," in *Computational Strategies for Spectroscopy : From Small Molecules to Nanosystems*, edited by V. Barone (John Wiley & Sons, Chichester, UK, 2011), pp. 361–443.
[4] L. González, D. Escudero, and L. Serrano-Andrés, ChemPhysChem **13**, 28 (2012).
[5] D. Jacquemin, E. A. Perpete, I. Ciofini, and C. Adamo, Acc. Chem. Res. **42**, 326 (2009).
[6] A. Dreuw and M. Head-Gordon, Chem. Rev. **105**, 4009 (2005).
[7] T. Yoshikawa, M. Kobayashi, A. Fujii, and H. Nakai, J. Phys. Chem. B **117**, 5565 (2013).
[8] A. Charaf-Eddin, A. Planchat, B. Mennucci, C. Adamo, and D. Jacquemin, J. Chem. Theory Comput. **9**, 2749 (2013).
[9] G. N. Ten, A. A. Yakovleva, M. K. Berezin, and V. I. Baranov, Opt. Spectrosc. **114**, 590, (2013).
[10] Y. Kawashima, S. Yamamoto, T. Sakata, H. Nakano, K. Nishiyama, and R. Akiyama, J. Phys. Soc. Jpn. **81**, SA024 (2012).
[11] D. Sundholm, S. Taubert, and F. Picchierri, Phys. Chem. Chem. Phys. **12**, 2751 (2010).
[12] E. Benassi and P. S. Sherin, Int. J. Quantum Chem. **111**, 3799 (2011).
[13] R. Improta, G. Scalmani, M. J. Frisch, and V. Barone, J. Chem. Phys. **127**, 074504 (2007).
[14] P. R. Callis, A. Petrenko, P. L. Muin, and J. R. Tusell, J. Phys. Chem. B **111**, 10335 (2007).
[15] B. M. Wong, M. Piacenza, and F. Della Sala, Phys. Chem. Chem. Phys. **11**, 4498 (2009).
[16] M. Pastore and F. De Angelis, J. Phys. Chem. Lett. **3**, 2146 (2012)
[17] S. Pistolesi, A. Sinicropi, R. Pogni, R. Basosi, N. Ferre', and M. Olivucci, J. Phys. Chem. B **113**, 16082 (2009).
[18] N. A. Murugan, P. C. Jha, Z. Rinkevicius, K. Ruud, and H. Ågren, J. Chem. Phys. **132**, 234508 (2010).
[19] S. Carlotto, A. Polimeno, C. Ferrante, C. Benzi, and V. Barone, J. Phys. Chem. B **112**, 8106 (2008).
[20] S. Vukovic, S. Corni, and B. Mennucci, J. Phys. Chem. C **113**, 121 (2009).
[21] G. F. Schröder, U. Alexiev, and H. Grubmüller, Biophys. J. **89**, 3757 (2005).
[22] C. A. Bortolotti, A. Amadei, M. Aschi, M. Borsari, S. Corni, M. Sola, and I. Daidone, J. Am. Chem. Soc. **134**, 13670 (2012).
[23] A. Amadei, F. Marinelli, M. D'Abramo, M. D'Alessandro, M. Anselmi, A. Di Nola, and M. Aschi, J. Chem. Phys. **122**, 124506 (2005).
[24] A. Amadei, I. Daodone, L. Zanetti-Polzi, and M. Aschi, Theor. Chem. Acc. **129**, 31–43 (2011).
[25] M. Aschi, A. Fontana, E. Di Meo, C. Zazza, and A. Amadei, J. Phys. Chem. B **114**, 1915 (2010).
[26] P. de Sainte Claire, J. Phys. Chem. B **110**, 7334 (2006).
[27] V. Barone, J. Bloino, S. Monti, A. Pedone, and G. Prampolini, Phys. Chem. Chem. Phys. **13**, 2160 (2011).
[28] M. Aschi, R. Spezia, A. Di Nola, and A. Amadei, Chem. Phys. Lett. **344**, 374 (2001).
[29] A. Amadei, M. D'Alessandro, M. D'Abramo, and M. Aschi, J. Chem. Phys. **130**, 084109 (2009).
[30] D. Jacquemin, A. Planchat, C. Adamo, and B. Mennucci, J. Chem. Theory and Comput. **8**, 2359 (2012).
[31] L. Goerigk and S. Grimme, J. Chem. Phys. **132**, 184103 (2010).
[32] M. Aschi, A. Amadei, A. Pellegrino, N. Perin, and R. Po, Theor. Chem. Acc. **131**, 1177 (2012).
[33] A. Warshel and M. Levitt, J. Mol. Biol. **103**, 227 (1976).
[34] M. W. van der Kamp, and A. J. Mulholland, Biochemistry **52**, 2708 (2013).
[35] L. M. Beechem, E. Gratton, M. Ameloot, J. R. Knutson, and L. Brand, in *Topics in Fluorescence Spectroscopy, Vol. 2: Principles*, edited by J. R. Lakowicz (Plenum Press, New York, 1991), p. 241.
[36] J. R. Lakowicz, *Principles of Fluorescence Spectroscopy* (Kluwer Academic Publishers, New York, 1999).
[37] B. Pispisa, C. Mazzuca, A. Palleschi, L. Stella, M. Venanzi, M. Wakselman, J.-P. Mazaleyrat, M. Rainaldi, F. Formaggio, and C. Toniolo, Chem. Eur. J. **9**, 4084 (2003).

[38]G. Bocchinfuso, C. Mazzuca, A. Palleschi, R. Pizzoferrato, and P. Tagliatesta, J. Phys. Chem. A 2009, **113**, 14887 (2009).
[39]D. S. Karpovic, and G. J. Blanchard, J. Phys. Chem. **99**, 3951 (1995).
[40]A. Nakajima, Bull. Chem. Soc. Jpn. **44**, 3272 (1971).
[41]D. F. Eaton, Pure Appl. Chem. **60**, 1107 (1988).
[42]C. Oostenbrink, A. Villa, A. E. Mark, and W. F. van Gunsteren, J. Comput. Chem. **25**, 1656 (2004).
[43]H. J. C. Berendsen, J. P. M. Postma, W. F. van Gunsteren, A. Di Nola, and J. R. Haak, J. Chem. Phys. **81**, 3684 (1984).
[44]J. D. Evans and G. P. Morriss, *Statistical Mechanics of Non-Equilibrium Liquids*, Theoretical Chemistry Monograph Series (Academic Press, London, 1990).
[45]B. Hess, H. Bekker, H. J. C. Berendsen, and J. C. E. M. Frajie, J. Comput. Chem. **18**, 1463 (1997).
[46]T. A. Darden, D. M. York, and L. G. Pedersen, "Particle mesh Ewald: An *N*log(*N*) method for Ewald sums in large systems," J. Chem. Phys. **98**, 10089 (1993).
[47]D. Van der Spoel, A. R. van Buren, E. Apol, P. J. Meulenhoff, D. P. Tieleman, A. L. T. M. Sijbers, R. van Drunen, and H. J. C. Berendsen, Gromacs User Manual version 1.3, 1996.
[48]A. Amadei, A. B. M. Linssen, and H. J. C. Berendsen, "Essential dynamics of proteins," Proteins: Struct., Funct., Genet. **17**, 412 (1993).
[49]A. D. Becke, "A new mixing of Hartree-Fock and local density-functional theories," J. Chem. Phys. **98**, 1372 (1993).
[50]C. Lee, W. Yang, and R. G. Parr, "Development of the Colle-Salvetti correlation-energy formula into a functional of the electron density," Phys. Rev. B **37**, 785 (1998).
[51]M. W. Schmidt, K. K. Baldridge, J. A. Boatz, S.-T. Elbert, M. S. Gordon, J. H. Jensen, S. Koseki, N. Matsunaga, K. A. Nguyen, S. Su, T. L. Windus, M. Dupuis, and J. A. Montgomery, J. Comput. Chem. **14**, 1347 (1993).
[52]E. K. U. Gross, J. F. Dobson, and M. Petersilka, Top. Curr. Chem. **181**, 81 (1996).
[53]DALTON, A molecular electronic structure program written by T. Helgaker, H. J. A. Jensen, P. Jørgensen, J. Olsen, K. Ruud, H. Ågren, T. Andersen, K. L. Bak, V. Bakken, O. Christiansen *et al.*
[54]K. Gustav, U. Kempka, and J. Sühnel, Chem. Phys. Lett. **71**, 280 (1980).
[55]B. Pispisa, C. Mazzuca, A. Palleschi, L. Stella, M. Venanzi, F. Formaggio, A. Polese, and C. Toniolo, J. Pept. Sci. **55**, 425 (2000).